

Figure 1. Diagram illustrating the workflow of a network-based, deep-learning methodology (termed CoV-KGE) for drug repurposing in COVID-19. Specifically, a comprehensive knowledge graph that contains 15 million edges across 39 types of relationships connecting drugs, diseases, genes, pathways, expressions, and others by incorporating data from 24 million PubMed publications and DrugBank (Table S2). Subsequently, a deep-learning approach (RotatE in DGL-KE) was used to prioritize high-confidence candidate drugs for COVID-19 under Amazon supercomputing resources (cf. Methods and Materials). Finally, all CoV-KGE predicted drug candidates were future-validated by three gene expression data sets in SARS-CoV-1-infected human cells and one proteomics data set in SARS-CoV-2 infected human cells.

63 Prior knowledge of networks from the large scientific corpus
64 of publications offers a deep biological perspective for
65 capturing the relationships between drugs, genes, and diseases
66 (including COVID-19), yet extracting connections from a
67 large-scale repository of structured medical information is
68 challenging. In this study, we present the state-of-the-art
69 knowledge-graph-based, deep-learning methodologies for the
70 rapid discovery of drug candidates to treat COVID-19 from 24
71 million PubMed publications (Figure 1). Via systematic
72 validation using transcriptomics and proteomics data generated

from SARS-CoV-2-infected human cells and the ongoing 73
clinical trial data, we successfully identified 41 drug candidates 74
that can be further tested in large-scale randomized control 75
trials for the potential treatment of COVID-19. 76

■ METHODS AND MATERIALS 77

Pipeline of CoV-KGE 78

Here we present a knowledge-graph (KG)-based, deep- 79
learning methodology for drug repurposing in COVID-19, 80

81 termed CoV-KGE (Figure 1). Our method uses DGL-KE,
82 developed by our Amazon's AWS AI Laboratory,¹⁷ to
83 efficiently learn embeddings of large KGs. Specifically, we
84 construct a KG from 24 million PubMed publications¹⁸ and
85 DrugBank,¹⁹ including 15 million edges across 39 types of
86 relationships connecting drugs, diseases, genes, anatomies,
87 pharmacologic classes, gene/protein expression, and others (cf.
88 Tables S1 and S2). In this KG, we represent the Coronaviruses
89 (CoVs) by assembling multiple types of known CoVs,
90 including SARS-CoV-1 and MERS-CoV, as described in our
91 recent study.⁹

92 We next utilized DGL-KE's knowledge graph embedding
93 (KGE) model, RotatE,²⁰ to learn representations of the entities
94 (e.g., drugs and targets) and relationships (e.g., inhibition
95 relation between drugs and targets) in an informative, low-
96 dimensional vector space. In this space, each relationship type
97 (e.g., antagonists or agonists) is defined as a rotation from the
98 source entity (e.g., hydroxychloroquine) to the target entity
99 (e.g., toll-like receptor 7/9 (TLR7/9)).

100 Constructing the Knowledge Graph

101 In this study, we constructed a comprehensive KG from Global
102 Network of Biomedical Relationships (GNBR)¹⁸ and
103 DrugBank.¹⁹ First, from GNBR, we included in the KG
104 relations corresponding to drug–gene interactions, gene–gene
105 interactions, drug–disease associations, and gene–disease
106 associations. Second, from the DrugBank database,¹⁹ we
107 selected the drugs whose molecular mass is >230 Da and
108 also exist in GNBR, resulting in 3481 FDA-approved and
109 clinically investigational drugs. For these drugs, we included in
110 the KG relationships corresponding to the drug–drug
111 interactions and the drug side-effects, drug anatomical
112 therapeutic chemical (ATC) codes, drug mechanisms of
113 action, drug pharmacodynamics, and drug-toxicity associations.
114 Third, we included the experimentally discovered CoV–gene
115 relationships from our recent work in the KG.⁹ Fourth, we
116 treated the COVID-19 context by assembling known genes/
117 proteins associated with CoVs (including SARS-CoV and
118 MERS-CoV) as a comprehensive node of CoVs and rewired
119 the connections (edges) from genes and drugs. The resulting
120 KG contains four types of entities (drug, gene, disease, and
121 drug side information), 39 types of relationships (Table S1),
122 145 179 nodes, and 15 018 067 edges (Table S2).

123 Knowledge Graph Embedding Model RotatE

124 Models for computing KGEs learn vectors for each of the
125 entities and each of the relation types so that they satisfy
126 certain properties. In our work, we learned these vectors using
127 the RotatE model.²⁰ Given an edge in the KG represented by
128 the triplet (head entity, relation type, and tail entity), RotatE
129 defines each relation type as a rotation from the head entity to
130 the tail entity in the complex vector space. Specifically, if h and
131 t are the vectors corresponding to the head and tail entities,
132 respectively, and r is the vector corresponding to the relation
133 type, then RotatE tries to minimize the distance

$$134 \quad d_r(h, t) = \|h \otimes r - t\| \quad (1)$$

135 where \otimes denotes the Hadamard (element-wise) product.

136 To minimize the distance between the head and the tail
137 entities of the existing triplets (positive examples) and
138 maximize the distance among the nonexisting triplets (negative
139 examples), we use the loss function

$$L = -\log \sigma(\gamma - d_r(h, t)) - \sum_{i=1}^n p(h_i, r, t_i) \\ \log \sigma(d_r(h_i, t_i) - \gamma) \quad (2) \quad 140$$

where σ is sigmoid function, γ is a margin hyperparameter with
141 $\gamma > 0$, (h, r, t) is a negative triplet, and $p(h, r, t)$ is the
142 probability of occurrence of the corresponding negative
143 sample. 144

145 Details of DGL-KE Package

DGL-KE¹⁷ is a high-performance, easy-to-use, and scalable
146 package for learning large-scale KGEs with a set of popular
147 models including TransE, DistMult, ComplEx, and RotatE. It
148 includes various optimizations that accelerate training on KGs
149 with millions of nodes and billions of edges using multi-
150 processing, multi-GPU (graphics processor unit), and dis-
151 tributed parallelism. DGL-KE is able to compute the RotatE-
152 based embeddings of our KG in ~40 min on an EC2 instance
153 with 8 GPUs under Amazon's AWS computing resources. 154

155 Experimental Settings

We divide the triplets (e.g., a relationship among drug,
156 treatment, and disease) into a training set, validation set, and
157 test set in a 7:1:2 manner. We selected the embedding
158 dimensionality of $\text{dim} = 200$ for nodes and relations. The
159 RotatE is trained for 16 000 epochs with a batch size 1024 and
160 0.1 as the learning rate. We choose $\gamma = 12$ as the margin of
161 the optimization function. 162

163 Gene-Set Enrichment Analysis

Gene set enrichment analysis was performed to further validate
164 the predicted drug candidates from CoV-KGE. The goal of the
165 gene set enrichment analysis was to identify drugs that can
166 reverse the cellular changes (transcriptome or proteome levels)
167 that result from virus infection. Four differential expression
168 data sets were collected, including two transcriptome data sets
169 from SARS-CoV patients' peripheral blood²¹ (GSE1739) and
170 Calu-3 cells²² (GSE33267), one transcriptome data set of
171 Calu-3 cells infected by MERS-CoV²³ (GSE122876), and one
172 proteome data set of human Caco-2 cells infected with SARS-
173 CoV-2.²⁴ These four data sets were used as the gene signatures
174 for the viral infections. For the drugs, we retrieved the
175 Connectivity Map (CMap) database²⁵ containing the gene
176 expression in cells treated with various drugs. An enrichment
177 score (ES) for each CoV signature data set was calculated
178 using a previously described method²⁶ 179

$$ES = \begin{cases} ES_{\text{up}} - ES_{\text{down}}, & \text{sgn}(ES_{\text{up}}) \neq \text{sgn}(ES_{\text{down}}) \\ 0, & \text{else} \end{cases} \quad (3) \quad 180$$

ES_{up} and ES_{down} indicate the ES values for the up- and down-
181 regulated genes from the CoV gene signature data set. To
182 compute $ES_{\text{up/down}}$, we first calculated $a_{\text{up/down}}$ and $b_{\text{up/down}}$ as
183

$$a = \max_{1 \leq j \leq s} \left(\frac{j}{s} - \frac{V(j)}{r} \right) \quad (4) \quad 184$$

$$b = \max_{1 \leq j \leq s} \left(\frac{V(j)}{r} - \frac{j-1}{s} \right) \quad (5) \quad 185$$

where $j = 1, 2, \dots, s$ are the genes from the CoV signature data
186 set sorted in ascending order using the gene profiles of the
187 drug being computed. $V(j)$ denotes the rank of j , where $1 \leq$
188 $V(j) \leq r$, with r being the total number of genes (12 849) from
189

the CMap database. Next, $ES_{\text{up/down}}$ is set to $a_{\text{up/down}}$ if $a_{\text{up/down}} > b_{\text{up/down}}$ and is set to $-b_{\text{up/down}}$ if $b_{\text{up/down}} > a_{\text{up/down}}$. Permutation tests are repeated 100 times to quantify the significance of the ES score. In each repeat, the same number of up- and down- expressed genes as the CoV signature data set was randomly generated. $ES > 0$ and $P < 0.05$ are considered significantly enriched. The number of significantly enriched data sets is used as the final result for a certain drug.

Performance Evaluation

We introduced the area under the receiver operating characteristic (ROC) curve (AUROC) and several evaluation metrics for evaluating the performance of drug–target interaction prediction. The AUROC²⁷ is the global performance. The ROC curve is obtained by calculating the true-positive rate (TPR) and the false-positive rate (FPR) via varying cutoffs.

RESULTS

High Performance of CoV-KGE

After mapping drugs, CoVs, and the treatment relationships to a complex vector space using RotatE, the top 100 most relevant drugs were selected as candidates for CoVs in the treatment relation space (Figure S1). Using the ongoing COVID-19 trial data (<https://covid19-trials.com/>) as a validation set, CoV-KGE has a larger AUROC (AUROC = 0.85, Figure 2) for identifying repurposable drugs for COVID-19.

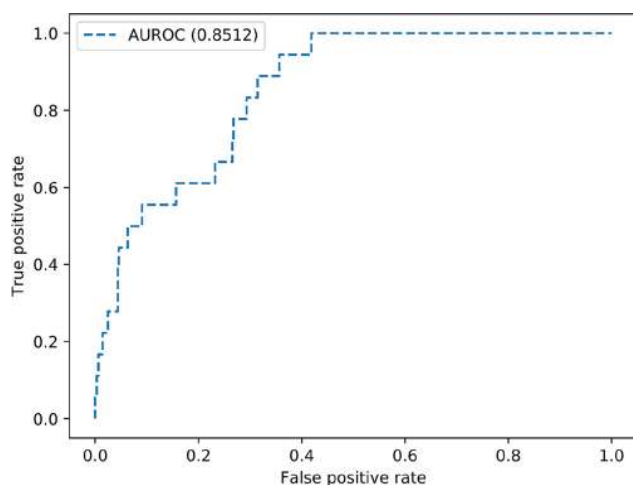


Figure 2. Performance of CoV-KGE in the prediction of drug candidates for COVID-19. Drugs in the ongoing COVID-19 trial data (<https://covid19-trials.com/>) were used as the validation set. AUROC, area under the ROC curve.

We next employ t-SNE (t-distributed stochastic neighbor embedding algorithm²⁸) to further investigate the low-dimensional node representation learned by CoV-KGE. Specifically, we projected drugs grouped by the first level of the Anatomical Therapeutic Chemical (ATC) classification systems code onto a 2D space. Figure 3A indicates that CoV-KGE is able to distinguish 14 types of drugs grouped by ATC codes, which is consistent with a high AUROC value of 0.85 (Figure 2).

We further validated the top candidate drugs using an enrichment analysis of drug–gene signatures and SARS-CoV-induced transcriptomics and proteomics data in human cell

lines (cf. Methods and Materials). Specifically, we analyzed three transcriptomic data sets in SARS-CoV-1-infected human cell lines and one proteomics data set in SARS-CoV-2-infected human cell lines. In total, we obtained 41 repositioned drug candidates (Table 1) using subject-matter expertise based on a combination of factors: (i) the strength of the CoV-KGE predicted score, (ii) the availability of clinical evidence from ongoing COVID-19 trials, and (iii) the availability and strength of enrichment analyses from SARS-CoV-1/2-affected human cell lines. Among the 41 candidate drugs, 9 drugs are or have been under clinical trials for COVID-19, including thalidomide, methylprednisolone, ribavirin, umifenovir, tetrandrine, suramin, dexamethasone, lopinavir, and azithromycin (Figure 3A and Table 1). We excluded chloroquine and hydroxychloroquine from our ongoing clinical trial list based on recently controversial reports.^{29,30}

Discovery of Drug Candidates for COVID-19 Using CoV-KGE

We next turned to highlight three types of predicted drugs for COVID-19, including anti-inflammatory agents (dexamethasone, indomethacin, and melatonin), selective estrogen receptor modulators (SERMs), and antiparasitics (Figure 3).

Anti-inflammatory Agents. Given the well-described lung pathophysiological characteristics and immune responses (cytokine storms) of severe COVID-19 patients, drugs that dampen the immune responses may offer effective treatment approaches for COVID-19.^{31,32} As shown in Figure 3A, we computationally identified multiple anti-inflammatory agents for COVID-19, including dexamethasone, indomethacin, and melatonin. Indomethacin, an approved cyclooxygenase (COX) inhibitor, has been widely used for its potent anti-inflammatory and analgesic properties.³³ Indomethacin has been reported to have antiviral properties, including SARS-CoV-1³³ and SARS-CoV-2.³⁴ Importantly, a preliminary *in vivo* observation showed that oral indomethacin (1 mg/kg body weight daily) reduced the recovery time of SARS-CoV-2-infected dogs.³⁴ Melatonin plays a key role in the regulation of the human circadian rhythm that alters the translation of thousands of genes, including melatonin-mediated anti-inflammatory and immune-related effects for COVID-19. Melatonin has various antiviral activities by suppressing multiple inflammatory pathways^{35,36} (i.e., IL6 and IL-1 β); these inflammatory effects are directly relevant given the well-described lung pathophysiological characteristics of severe COVID-19 patients. Melatonin's mechanism of action may also help to explain the epidemiologic observation that children, who have naturally high melatonin levels, are relatively resistant to COVID-19 disease manifestations, whereas older individuals, who have decreasing melatonin levels with age, are a very high-risk population.³⁷ In addition, exogenous melatonin administration may be of particular benefit to older patients given the aging-related reduction of endogenous melatonin levels and the vulnerability of older individuals to the lethality of SARS-CoV-2.³⁷

Dexamethasone is a U.S. FDA-approved glucocorticoid receptor (GR) agonist for a variety of inflammatory and autoimmune conditions, including rheumatoid arthritis, severe allergies, asthma, chronic obstructive lung disease, and others.³⁸ Glucocorticoid medications have been used in patients with MERS-CoV and SARS-CoV-1 infections.³⁹ As shown in Figure 3A, dexamethasone is the fourth predicted drug among 41 candidates. The Randomized Evaluation of

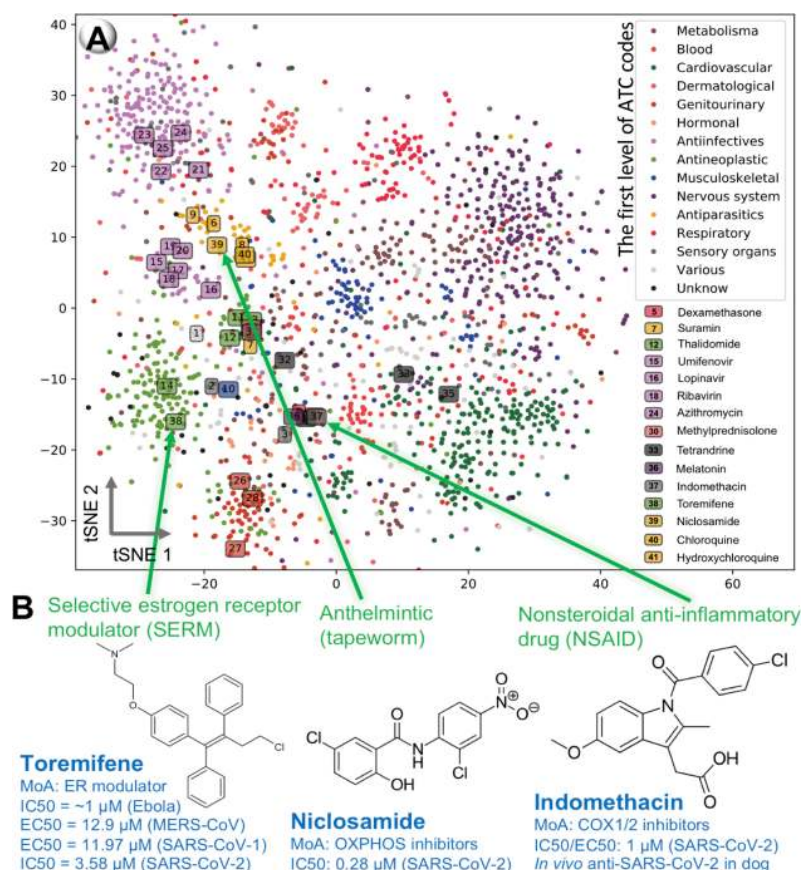


Figure 3. Diagram illustrating the landscape of CoV-KGE-predicted repurposable drugs for COVID-19. (A) Visualization of the drug vector learned by the knowledge graph embedding using t-SNE (t-distributed stochastic neighbor embedding algorithm²⁸). 2D representation of the learned vectors for 14 types of drugs grouped by the first level of the Anatomical Therapeutic Chemical (ATC) classification system codes. Semantically similar ATC drugs are mapped to nearby representations. We highlighted 11 drugs that are under clinical trials for COVID-19. (B) Three highlighted drugs (toremifene, niclosamide, and indomethacin) having striking *in vitro* antiviral activities across Ebola virus,^{42,43} MRES-CoV,⁴⁴ SARS-CoV-1,⁴⁵ and SARS-CoV-2.⁴⁶

290 COVID-19 therapy (RECOVERY, [ClinicalTrials.gov](https://clinicaltrials.gov/ct2/show/study/NCT04381936) Identifier: NCT04381936) trial showed that dexamethasone reduced
 291 mortality by one-third in patients requiring ventilation and by
 292 one-fifth in individuals requiring oxygen,⁴⁰ yet dexamethasone
 293 did not reduce death in COVID-19 patients not receiving
 294 respiratory support.⁴⁰

296 **Selective Estrogen Receptor Modulators.** An over-
 297 expression of the estrogen receptor has played a crucial role in
 298 inhibiting viral replication and infection.⁴¹ Several SERMs,
 299 including clomifene, bazedoxifene, and toremifene, are
 300 identified as promising candidate drugs for COVID-19 (Figure
 301 3A and Table 1). Toremifene, the first generation of the
 302 nonsteroidal SERM, was reported to block various viral
 303 infections at low micromolar concentration, including Ebola
 304 virus,^{42,43} MRES-CoV,⁴⁴ SARS-CoV-1,⁴⁵ and SARS-CoV-2⁴⁶
 305 (Figure 3B). Toremifene prevents fusion between the viral and
 306 endosomal membranes by interacting with and destabilizing
 307 the virus glycoprotein and eventually blocking replications of
 308 the Ebola virus.⁴² The underlying antiviral mechanisms of
 309 SARS-CoV-1 and SARS-CoV-2 for toremifene remain unclear
 310 and are currently being investigated. Toremifene has been
 311 approved for the treatment of advanced breast cancer⁴⁷ and
 312 has also been studied in men with prostate cancer (~1500
 313 subjects) with reasonable tolerability.⁴⁸ Toremifene is 99%
 314 bound to plasma protein with good bioavailability and typically

orally administered at a dosage of 60 mg.⁴⁹ In summary, toremifene is a promising candidate drug with ideal
 316 pharmacokinetics properties to be directly tested in COVID-
 317 19 clinical trials.

319 **Antiparasitics.** Despite the lack of strong clinical evidence,
 320 hydroxychloroquine and chloroquine phosphate, two approved
 321 antimalarial drugs, were authorized by the U.S. FDA for the
 322 treatment of COVID-19 patients using emergency use
 323 authorizations (EUs).² In this study, we identified that
 324 both hydroxychloroquine and chloroquine are among the
 325 predicted candidates for COVID-19 (Figure 3A and Table 1).
 326 Between the two, hydroxychloroquine's *in vitro* antiviral
 327 activity against SARS-CoV-2 is stronger than that of
 328 chloroquine (hydroxychloroquine: 50% effective concentration
 329 (EC_{50}) = 6.14 μM , whereas for chloroquine: EC_{50} = 23.90
 330 μM).⁵⁰ Hydroxychloroquine and chloroquine are known to
 331 increase the pH of endosomes, which inhibits membrane
 332 fusion, a required mechanism for viral entry (including SARS-
 333 CoV-2) into the cell.¹⁹ Although chloroquine and hydroxy-
 334 chloroquine are relatively well tolerated, several adverse effects
 335 (including QT prolongation) limit their clinical use for
 336 COVID-19 patients, especially for patients with pre-existing
 337 cardiovascular disease or diabetes.^{10,51–53} A recent observa-
 338 tional study reported that hydroxychloroquine administration
 339 was not associated with either a greatly lowered or an increased

Table 1. Lists of the Selected 41 Top Drugs with the Potential to Treat COVID-19⁴

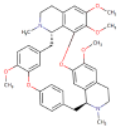
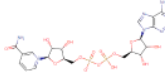
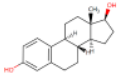
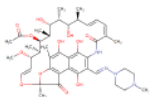
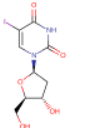
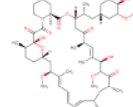
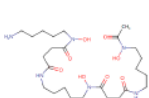
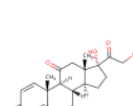
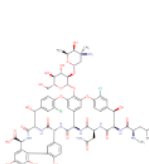
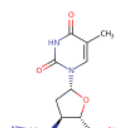
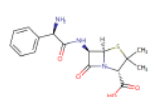
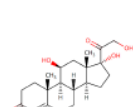
Drug Name	Enrichment analysis	Structure	Category	PubMed or Clinic trial id
Tetrandrine*	3		Adenine Nucleotides	<u>NCT04308317</u>
Nadide	4		Adenine Nucleotides	27134728
Estradiol	4		Adrenal Cortex Hormones	28373583 32052466 32199468
Rifampicin	3		Anti-Bacterial Agents	15227635 10517189 28683463
Idoxuridine	4		Anti-Infective Agents	31216912 30937274
Sirolimus	4		Anti-Bacterial Agents	29143192 25487801 32194980 32161092
Deferoxamine	3		Chelating Agents	6954069 24323450 25535360 16542729
Prednisone	3		Adrenal Cortex Hormones	16968120 32043983 29143192 16675038
Vancomycin	3		Anti-Bacterial Agents	12877785 25828287 26953343 29143192
Zidovudine	3		Anti-HIV Agents	31925415 29161116 15200845 28148787
Ampicillin	3		Anti-Bacterial Agents	15356814 23978488 29227752
Hydrocortisone	3		11- Hydroxycorticoste roids	27585965 15647850 15494274

Table 1. continued

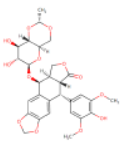
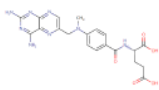
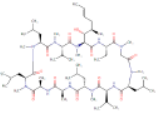
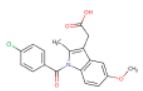
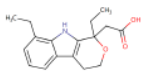
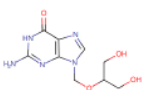
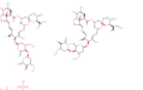
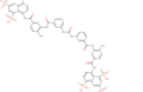
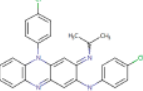
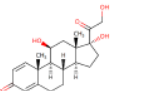
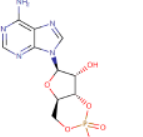
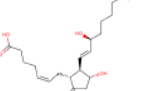
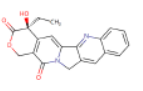
Drug Name	Enrichment analysis	Structure	Category	PubMed or Clin trial id
Etoposide	3		Antineoplastic Agents	28817732 26365771 32194944 32113509
Methotrexate	3		Abortifacient Agents	2805607 29496347 25084201 29772254
Cyclosporine	3		Agents causing hyperkalemia	23620378 27097824 23396219 17302372
Indomethacin	3		Analgesics	25856684 24096239 17555580 30581611
Etodolac	2		Agents causing hyperkalemia	32105468 30206897 32023685
Ganciclovir	2		Anti-Infective Agents	15200845 32169119 32251768
Ivermectin	2		Agrochemicals	24841269
Suramin*	2		Acids	CHICTR2000030016
Clofazimine	2		Anti-Infective Agents	30202770
Prednisolone	2		Adrenal Cortex Hormones	16542729 29143192 16968120
Cyclic adenosine monophosphate	2		Adenine Nucleotides	24453361
Dinoprostone	2		Biological Factors	30315411 11878905
Camptothecin	2		Antineoplastic Agents	

Table 1. continued

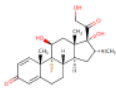
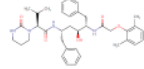
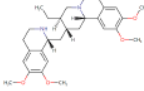
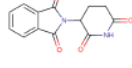
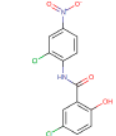
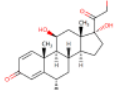
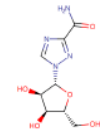
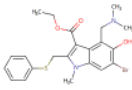
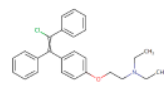
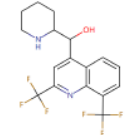
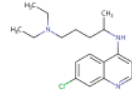
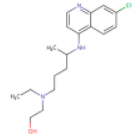
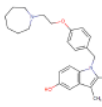
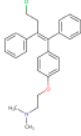
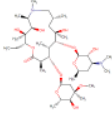
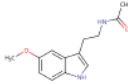
Drug Name	Enrichment analysis	Structure	Category	PubMed or Clin trial id
Dexamethasone*	2		Adrenal Cortex Hormones	NCT04325061
Lopinavir*	2		Anti-Infective Agents	CHICTR2000029468 32251767
Emetine	1		Agents Causing Muscle Toxicity	29143192 32245264 30918074
Thalidomide*	1		Acids, Carbocyclic	NCT04273529
Nicosamide	1		Agrochemicals	15215127 32125140 31852899
Methylprednisolone*	1		Adrenal Cortex Hormones	NCT04323592
Ribavirin*	1		Anti-Infective Agents	CHICTR2000030922
Umifenovir*	1		Antiviral Agents	NCT04252885
Clomifene	1		Clomiphene	25256397 30284220 19821295
Mefloquine	1		Anti-Infective Agents	32149769 29143192 32127666
Chloroquine	0		Agents Causing Muscle Toxicity	32194981
Hydroxychloroquine	0		Anti-Infective Agents	32194981

Table 1. continued

Drug Name	Enrichment analysis	Structure	Category	PubMed or Clin trial id
Bazedoxifene	0		Bone Density Conservation Agents	30852762 31587108
Toremifene	0		Anti-Estrogens	24841273 29143192 32194980
Azithromycin*	0		Anti-Bacterial Agents	<u>NCT04332107</u>
Melatonin	-		Antioxidants	32217117 32194980 29769094

*Note: Drugs marked with * are in clinical trials. All predicted drugs are freely available at <https://github.com/ChengF-Lab/CoV-KGE>. Enrichment scores (ESs) indicate the number of significantly enriched data sets for the drug.

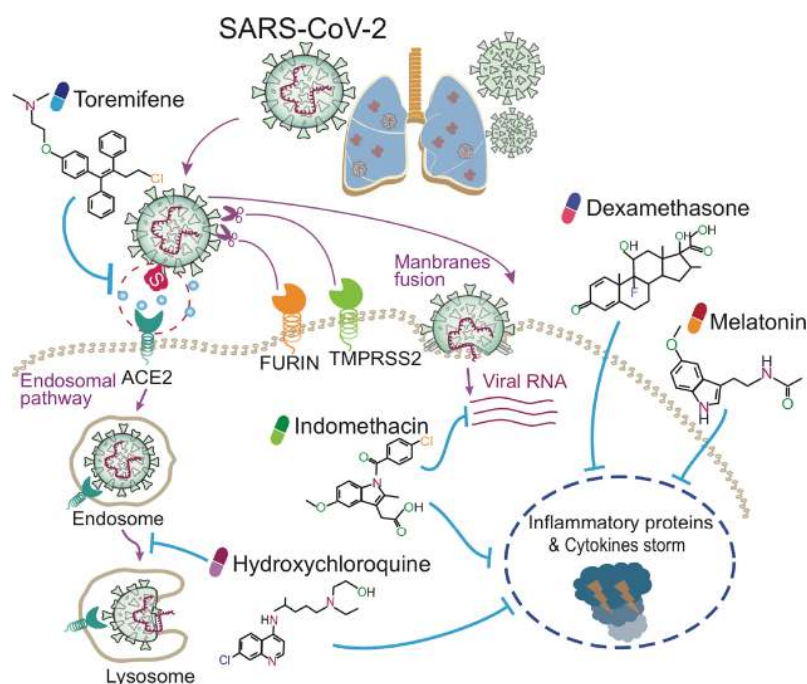


Figure 4. Proposed mechanism-of-action model that combines antiviral and anti-inflammatory agents for the potential treatment of COVID-19. Toremifene, a selective estrogen receptor modulator approved by the U.S. FDA for the treatment of advanced breast cancer, has shown various antiviral activities across Ebola virus,^{42,43} MRES-CoV,⁴⁴ SARS-CoV-1,⁴⁵ and SARS-CoV-2.⁴⁶ Melatonin is a synthesized hormone with ~2.5 billion years history. Given the well-described lung injury characteristics of severe COVID-19 by multiple inflammatory pathways,^{35,36} dexamethasone, indomethacin, and melatonin are candidate anti-inflammatory agents for the treatment of patients with COVID-19 (Figure 3A). Thus combining antiviral (toremifene or hydroxychloroquine) and anti-inflammatory agents (dexamethasone, indomethacin, or melatonin) may provide an effective treatment for COVID-19, as demonstrated in ongoing COVID-19 trials (remdesivir plus baricitinib, [clinicalTrials.gov](https://clinicaltrials.gov) Identifier: NCT04373044). ACE2, Angiotensin-converting enzyme 2; TMPRSS2, Transmembrane Serine Protease 2.

340 risk of the composite end point of intubation or death for
341 patients with COVID-19 who had been admitted to the
342 hospital.³⁵ As June 15, 2020, the U.S. FDA revoked the EUs
343 for hydroxychloroquine and chloroquine for the treatment of
344 COVID-19 patients.²⁹ As June 20, 2020, the National

Institutes of Health halted the clinical trial of hydroxychloro-
345 quine owing to the lack of clinical benefits.³⁰ Thus further
346 functional observations are urgently needed to investigate the
347 inconsistent results between *in vitro* antiviral activities and
348 clinical efficiency in the near future.
349

350 Niclosamide, an FDA-approved drug for the treatment of
351 tapeworm infestation, was recently identified to have a stronger
352 inhibitory activity on SARS-CoV-2 at the submicromolar level
353 ($IC_{50} = 0.28 \mu M$). Gassen et al. showed that niclosamide
354 inhibited SKP2 activity by enhancing autophagy and reducing
355 MERS-CoV replication as well.⁵⁴ Altogether, niclosamide may
356 be another drug candidate for COVID-19, which is warranted
357 to be investigated experimentally and further tested in
358 randomized controlled trials.

359 Given the up-regulation of systemic inflammation—in some
360 cases, culminating to a cytokine storm observed in severe
361 COVID-19 patients³¹—combination therapy with an agent
362 targeting inflammation (melatonin, dexamethasone, or in-
363 domethacin) and with direct antiviral effects (toremifene and
364 niclosamide) has the potential to lead to successful treatments
365 (Figure 4). Because of the aging-related reduction of
366 endogenous melatonin levels and the vulnerability of older
367 individuals to the lethality of SARS-CoV-2,³⁷ combining
368 exogenous melatonin administration and antiviral agents
369 (such as toremifene or niclosamide) may be of particular
370 benefit to older patients with COVID-19. Yet all computa-
371 tionally predicted drug candidates (Table 1) and proposed
372 drug combinations (Figure 4) must be validated experimen-
373 tally and be tested in randomized controlled trials. Several
374 combination antiviral and anti-inflammatory treatment trials
375 (remdesivir plus baricitinib) are underway for patients with
376 COVID-19 (clinicalTrials.gov Identifier: NCT04373044),
377 indicating the proof-of-concept of this combination therapy
378 for COVID-19.

379 ■ DISCUSSION

380 As COVID-19 patients flood hospitals worldwide, physicians
381 are trying to search for effective antiviral therapies to save lives.
382 Multiple COVID-19 vaccine trials are underway, yet it might
383 not be physically possible to make enough vaccines for
384 everyone in a short period of time. Furthermore, SARS-CoV-2
385 replicates poorly in multiple animals, including dogs, pigs,
386 chickens, and ducks, which limits preclinical animal studies.⁵⁵
387 To fight the emerging COVID-19 pandemic, we introduced
388 an integrative, network-based, deep-learning methodology to
389 discover candidate drugs for COVID-19, named CoV-KGE.
390 Via CoV-KGE, we built a comprehensive KG that includes 15
391 million edges across 39 types of relationships connecting drugs,
392 diseases, proteins/genes, pathways, and expressions from a
393 large scientific corpus of 24 million PubMed publications.
394 Using the ongoing COVID-19 trial data as a validation set, we
395 demonstrated that CoV-KGE had high performance in
396 identifying repurposable drugs for COVID-19, indicated by
397 the larger AUROC (AUROC = 0.85). Using Amazon's AWS
398 computing resources, we identified 41 high-confidence
399 repurposed drug candidates (including dexamethasone, in-
400 domethacin, niclosamide, and toremifene) for COVID-19,
401 which were validated by an enrichment analysis of gene
402 expression and proteomics data in SARS-CoV-2 infected
403 human cells. Altogether, this study offers a powerful, integrated
404 deep-learning methodology for the rapid identification of
405 repurposable drugs for the potential treatment of COVID-19.
406 We acknowledge several potential limitations in the current
407 study. Potential data noises generated from different
408 experimental approaches in large-scale publications may
409 influence the performance of the current CoV-KGE models.
410 The original data of GNBR contain the confidence values of
411 the relations between entities. However, we ignored the

weights so that we could directly apply the RotatE algorithm 412
because we tried to obtain the prediction result in a cheap 413
computing-cost way. In our future work, we will take these 414
confidence values into account and try to design a knowledge- 415
graph-embedding algorithm that can be used for a KG with 416
weighted relationships. The lack of dose-dependent profiles 417
and the biological perturbation of SARS-CoV-2 virus–host 418
interactions may generate a coupled interplay between adverse 419
and therapeutic effects. The integration of pharmacokinetics 420
data from animal models and clinical trials into our CoV-KGE 421
methodology could establish the causal mechanism and patient 422
evidence through which predicted drugs would have high 423
clinical benefits for COVID-19 patients without obvious 424
adverse effects in a specific dosage. 425

In summary, we presented CoV-KGE, a powerful, integrated 426
AI methodology that can be used to quickly identify drugs that 427
can be repurposed for the potential treatment of COVID-19. 428
Our approach can minimize the translational gap between 429
preclinical testing results and clinical outcomes, which is a 430
significant problem in the rapid development of efficient 431
treatment strategies for the COVID-19 pandemic. From a 432
translational perspective, if broadly applied, the network tools 433
developed here could help develop effective treatment 434
strategies for other emerging infectious diseases and other 435
emerging complex diseases as well. However, all predicted 436
drugs not used in clinical trials must be tested in randomized 437
clinical trials before being used in patients. 438

■ ASSOCIATED CONTENT

 439

Supporting Information

 440

The Supporting Information is available free of charge at 441
<https://pubs.acs.org/doi/10.1021/acs.jproteome.0c00316>. 442

Supplementary Figure 1. Diagram illustrating the 443
prioritization of drugs based on their distance to 444
COVID-19 in the treatment relation space. Supple- 445
mentary Table 1. Details of the five categories of 446
relationships in our KG. Supplementary Table 2. 447
Statistics of nodes (entity) and edges (relation) in our 448
KG (PDF) 449

■ AUTHOR INFORMATION

 450

Corresponding Authors

 451

George Karypis – AWS AI, East Palo Alto, California 94303, 452
United States; Department of Computer Science and 453
Engineering, University of Minnesota, Minneapolis, Minnesota 454
55455, United States; Email: karypis@umn.edu 455

Feixiong Cheng – Genomic Medicine Institute, Lerner Research 456
Institute, Cleveland Clinic, Cleveland, Ohio 44106, United 457
States; Department of Molecular Medicine, Cleveland Clinic 458
Lerner College of Medicine, Case Western Reserve University, 459
Cleveland, Ohio 44195, United States; Case Comprehensive 460
Cancer Center, Case Western Reserve University School of 461
Medicine, Cleveland, Ohio 44106, United States; orcid.org/0000-0002-1736-2847; Email: chengf@ccf.org 462
463

Authors

 464

Xiangxiang Zeng – School of Computer Science and 465
Engineering, Hunan University, Changsha 410012, China 466
Xiang Song – AWS Shanghai AI Lab, Shanghai 200335, China 467
Tengfei Ma – School of Computer Science and Engineering, 468
Hunan University, Changsha 410012, China 469

470 **Xiaoqin Pan** – School of Computer Science and Engineering,
471 Hunan University, Changsha 410012, China
472 **Yadi Zhou** – Genomic Medicine Institute, Lerner Research
473 Institute, Cleveland Clinic, Cleveland, Ohio 44106, United
474 States
475 **Yuan Hou** – Genomic Medicine Institute, Lerner Research
476 Institute, Cleveland Clinic, Cleveland, Ohio 44106, United
477 States
478 **Zheng Zhang** – AWS Shanghai AI Lab, Shanghai 200335,
479 China; New York University Shanghai, Shanghai 200122,
480 China
481 **Kenli Li** – School of Computer Science and Engineering, Hunan
482 University, Changsha 410012, China

483 Complete contact information is available at:
484 <https://pubs.acs.org/10.1021/acs.jproteome.0c00316>

485 Author Contributions

486 ◆X.Z. and X.S. are joint first authors on this work.

487 Notes

488 The authors declare no competing financial interest.
489 Source code and data can be downloaded from <https://github.com/ChengF-Lab/CoV-KGE>.
490

491 ACKNOWLEDGMENTS

492 We acknowledge support from the Amazon Cloud, for credits
493 to AWS ML Services. The therapeutics discussed in this study
494 are computationally predicted and are not currently approved
495 for the treatment of COVID-19. The content of this
496 publication does not necessarily reflect the views of the
497 Cleveland Clinic.

498 REFERENCES

499 (1) Dong, E.; Du, H.; Gardner, L. An interactive web-based
500 dashboard to track COVID-19 in real time. *Lancet Infect. Dis.* **2020**,
501 *20*, 533–534.
502 (2) Sanders, J. M.; Monogue, M. L.; Jodlowski, T. Z.; Cutrell, J. B.
503 Pharmacologic treatments for Coronavirus disease 2019 (COVID-
504 19): A Review. *JAMA* **2020**, *323* (18), 1824–1836.
505 (3) Avorn, J. The \$2.6 billion pill–methodologic and policy
506 considerations. *N. Engl. J. Med.* **2015**, *372* (20), 1877–9.
507 (4) Harrison, C. Coronavirus puts drug repurposing on the fast
508 track. *Nat. Biotechnol.* **2020**, *38* (4), 379–381.
509 (5) Cao, B.; Wang, Y.; Wen, D.; Liu, W.; Wang, J.; Fan, G.; Ruan, L.;
510 Song, B.; Cai, Y.; Wei, M.; Li, X.; Xia, J.; Chen, N.; Xiang, J.; Yu, T.;
511 Bai, T.; Xie, X.; Zhang, L.; Li, C.; Yuan, Y.; Chen, H.; Li, H.; Huang,
512 H.; Tu, S.; Gong, F.; Liu, Y.; Wei, Y.; Dong, C.; Zhou, F.; Gu, X.; Xu,
513 J.; Liu, Z.; Zhang, Y.; Li, H.; Shang, L.; Wang, K.; Li, K.; Zhou, X.;
514 Dong, X.; Qu, Z.; Lu, S.; Hu, X.; Ruan, S.; Luo, S.; Wu, J.; Peng, L.;
515 Cheng, F.; Pan, L.; Zou, J.; Jia, C.; Wang, J.; Liu, X.; Wang, S.; Wu, X.;
516 Ge, Q.; He, J.; Zhan, H.; Qiu, F.; Guo, L.; Huang, C.; Jaki, T.;
517 Hayden, F. G.; Horby, P. W.; Zhang, D.; Wang, C. A trial of lopinavir-
518 ritonavir in adults hospitalized with severe COVID-19. *N. Engl. J. Med.*
519 **2020**, *382* (19), 1787–1799.
520 (6) Hoffmann, M.; Kleine-Weber, H.; Schroeder, S.; Kruger, N.;
521 Herrler, T.; Erichsen, S.; Schiergens, T. S.; Herrler, G.; Wu, N. H.;
522 Nitsche, A.; Muller, M. A.; Drosten, C.; Pohlmann, S. SARS-CoV-2
523 cell entry depends on ACE2 and TMPRSS2 and is blocked by a
524 clinically proven protease inhibitor. *Cell* **2020**, *181* (2), 271–280.
525 (7) Gordon, D. E.; Jang, G. M.; Bouhaddou, M.; Xu, J.; Obernier, K.;
526 O’Meara, M. J.; Guo, J. Z.; Swaney, D. L.; Tummino, T. A.;
527 Huttenhain, R.; Kaake, R.; Richards, A. L.; Tutuncuoglu, B.; Foussard,
528 H.; Batra, J.; Haas, K.; Modak, M.; Kim, M.; Haas, P.; Polacco, B. J.;
529 Braberg, H.; Fabius, J. M.; Eckhardt, M.; Soucheray, M.; Brewer, M.;
530 Cakir, M.; McGregor, M. J.; Li, Q.; Naing, Z. Z. C.; Zhou, Y.; Peng,

S.; Kirby, I. T.; Melnyk, J. E.; Chorba, J. S.; Lou, K.; Dai, S. A.; Shen, 531
W.; Shi, Y.; Zhang, Z.; Barrio-Hernandez, I.; Memon, D.; Hernandez- 532
Armenta, C.; Mathy, C. J. P.; Perica, T.; Pilla, K. B.; Ganesan, S. J.; 533
Saltzberg, D. J.; Ramachandran, R.; Liu, X.; Rosenthal, S. B.; Calviello, 534
L.; Venkataramanan, S.; Lin, Y.; Wankowicz, S. A.; Bohn, M.; 535
Trenker, R.; Young, J. M.; Caverio, D.; Hiatt, J.; Roth, T.; Rathore, U.; 536
Subramanian, A.; Noack, J.; Hubert, M.; Roesch, F.; Vallet, T.; Meyer, 537
B.; White, K. M.; Miorin, L.; Agard, D.; Emerman, M.; Ruggero, D.; 538
Garc; Amp; iacute-Sastre, A.; Jura, N.; von Zastrow, M.; Taunton, J.; 539
Schwartz, O.; Vignuzzi, M.; d’Enfert, C.; Mukherjee, S.; Jacobson, M.; 540
Malik, H. S.; Fujimori, D. G.; Ideker, T.; Craik, C. S.; Floor, S.; Fraser, 541
J. S.; Gross, J.; Sali, A.; Kortemme, T.; Beltrao, P.; Shokat, K.; 542
Shoichet, B. K.; Krogan, N. J. A SARS-CoV-2 protein interaction map 543
reveals targets for drug repurposing. *Nature* **2020**, *583* (7816), 459– 544
468. 545
(8) Cheng, F.; Murray, J. L.; Zhao, J.; Sheng, J.; Zhao, Z.; Rubin, D. 546
H. Systems biology-based investigation of cellular antiviral drug 547
targets identified by gene-trap insertional mutagenesis. *PLoS Comput.* 548
Biol. **2016**, *12* (9), No. e1005074. 549
(9) Zhou, Y.; Hou, Y.; Shen, J.; Huang, Y.; Martin, W.; Cheng, F. 550
Network-based drug repurposing for novel coronavirus 2019-nCoV/ 551
SARS-CoV-2. *Cell Discov* **2020**, *6*, 14. 552
(10) Cheng, F.; Desai, R. J.; Handy, D. E.; Wang, R.; Schneeweiss, 553
S.; Barabasi, A. L.; Loscalzo, J. Network-based approach to prediction 554
and population-based validation of in silico drug repurposing. *Nat.* 555
Commun. **2018**, *9* (1), 2691. 556
(11) Cheng, F.; Kovacs, I. A.; Barabasi, A. L. Network-based 557
prediction of drug combinations. *Nat. Commun.* **2019**, *10* (1), 1197. 558
(12) Cheng, F.; Lu, W.; Liu, C.; Fang, J.; Hou, Y.; Handy, D. E.; 559
Wang, R.; Zhao, Y.; Yang, Y.; Huang, J.; Hill, D. E.; Vidal, M.; Eng, 560
C.; Loscalzo, J. A genome-wide positioning systems network 561
algorithm for in silico drug repurposing. *Nat. Commun.* **2019**, *10* 562
(1), 3476. 563
(13) Stokes, J. M.; Yang, K.; Swanson, K.; Jin, W.; Cubillos-Ruiz, A.; 564
Donghia, N. M.; MacNair, C. R.; French, S.; Carfrae, L. A.; Bloom- 565
Ackerman, Z. J. C.; et al. A deep learning approach to antibiotic 566
discovery. *Cell* **2020**, *180* (4), 688–702. 567
(14) Zeng, X.; Zhu, S.; Liu, X.; Zhou, Y.; Nussinov, R.; Cheng, F. 568
deepDR: a network-based deep learning approach to in silico drug 569
repositioning. *Bioinformatics* **2019**, *35* (24), 5191–5198. 570
(15) Zheng, S.; Li, Y.; Chen, S.; Xu, J.; Yang, Y. Predicting drug– 571
protein interaction using quasi-visual question answering system. *Nat.* 572
Mach. Intell. **2020**, *2* (2), 134–140. 573
(16) Zeng, X.; Zhu, S.; Lu, W.; Liu, Z.; Huang, J.; Zhou, Y.; Fang, J.; 574
Huang, Y.; Guo, H.; Li, L. J. C. S.; et al. Target identification among 575
known drugs by deep learning from heterogeneous networks. *Chem.* 576
Sci. **2020**, *11*, 1775–1797. 577
(17) Wang, M.; Yu, L.; Zheng, D.; Gan, Q.; Gai, Y.; Ye, Z.; Li, M.; 578
Zhou, J.; Huang, Q.; Ma, C.; Huang, Z.; Guo, Q.; Zhang, H.; Lin, H.; 579
Zhao, J.; Li, J.; Smola, A.; Zhang, Z. Deep Graph Library: Towards 580
Efficient and Scalable Deep Learning on Graphs. 2019, 581
arXiv:1909.01315 [cs.LG]. arXiv.org e-Print archive. <https://arxiv.org/pdf/1909.01315.pdf>. 582
(18) Percha, B.; Altman, R. B. J. B. A global network of biomedical 583
relationships derived from text. *Bioinformatics* **2018**, *34* (15), 2614– 584
2624. 585
(19) Wishart, D. S.; Feunang, Y. D.; Guo, A. C.; Lo, E. J.; Marcu, A.; 587
Grant, J. R.; Sajed, T.; Johnson, D.; Li, C.; Sayeeda, Z. J. N. a. r.; et al. 588
DrugBank 5.0: a major update to the DrugBank database for 2018. 589
Nucleic Acids Res. **2018**, *46* (D1), D1074–D1082. 590
(20) Sun, Z.; Deng, Z.-H.; Nie, J.-Y.; Tang, J. ROTate: Knowledge 591
Graph Embedding by Relational Rotation in Complex Space. 2019, 592
arXiv:1902.10197 [cs.LG]. arXiv.org e-Print archive. <https://arxiv.org/pdf/1902.10197.pdf>. 593
(21) Reghunathan, R.; Jayapal, M.; Hsu, L.-Y.; Chng, H.-H.; Tai, D.; 594
Leung, B. P.; Melendez, A. J. Expression profile of immune response 595
genes in patients with Severe Acute Respiratory Syndrome. *BMC* 596
Immunol. **2005**, *6* (1), 2. 597
598

- 599 (22) Josset, L.; Menachery, V. D.; Gralinski, L. E.; Agnihothram, S.;
600 Sova, P.; Carter, V. S.; Yount, B. L.; Graham, R. L.; Baric, R. S.; Katze,
601 M. G. Cell host response to infection with novel human coronavirus
602 EMC predicts potential antivirals and important differences with
603 SARS coronavirus. *mBio* **2013**, *4* (3), e00165–13.
- 604 (23) Yuan, S.; Chu, H.; Chan, J. F.-W.; Ye, Z.-W.; Wen, L.; Yan, B.;
605 Lai, P.-M.; Tee, K.-M.; Huang, J.; Chen, D.; Li, C.; Zhao, X.; Yang,
606 D.; Chiu, M. C.; Yip, C.; Poon, V. K.-M.; Chan, C. C.-S.; Sze, K.-H.;
607 Zhou, J.; Chan, I. H.-Y.; Kok, K.-H.; To, K. K.-W.; Kao, R. Y.-T.; Lau,
608 J. Y.-N.; Jin, D.-Y.; Perlman, S.; Yuen, K.-Y. SREBP-dependent
609 lipidomic reprogramming as a broad-spectrum antiviral target. *Nat.*
610 *Commun.* **2019**, *10* (1), 120.
- 611 (24) Bojkova, D.; Klann, K.; Koch, B.; Widera, M.; Krause, D.;
612 Ciesek, S.; Cinatl, J.; Munch, C. Proteomics of SARS-CoV-2-infected
613 host cells reveals therapy targets. *Nature* **2020**, *583*, 469.
- 614 (25) Lamb, J.; Crawford, E. D.; Peck, D.; Modell, J. W.; Blat, I. C.;
615 Wrobel, M. J.; Lerner, J.; Brunet, J. P.; Subramanian, A.; Ross, K. N.;
616 Reich, M.; Hieronymus, H.; Wei, G.; Armstrong, S. A.; Haggarty, S. J.;
617 Clemons, P. A.; Wei, R.; Carr, S. A.; Lander, E. S.; Golub, T. R. The
618 Connectivity Map: using gene-expression signatures to connect small
619 molecules, genes, and disease. *Science* **2006**, *313* (5795), 1929–35.
- 620 (26) Sirota, M.; Dudley, J. T.; Kim, J.; Chiang, A. P.; Morgan, A. A.;
621 Sweet-Cordero, A.; Sage, J.; Butte, A. J. Discovery and preclinical
622 validation of drug indications using compendia of public gene
623 expression data. *Sci. Transl. Med.* **2011**, *3* (96), 96ra77.
- 624 (27) Powers, D. M. Evaluation: from precision, recall and F-measure
625 to ROC, informedness, markedness and correlation. *J. Mach. Learn.*
626 *Technol.* **2011**, *2* (1), 37–63.
- 627 (28) van der Maaten, L.; Hinton, G. Visualizing data using t-SNE. *J.*
628 *Mach. Learn. Res.* **2008**, *9*, 2579–2605.
- 629 (29) U.S. FDA. Coronavirus (COVID-19) Update: FDA Revokes
630 Emergency Use Authorization for Chloroquine and Hydroxychloro-
631 quine. <https://www.fda.gov/news-events/press-announcements/coronavirus-covid-19-update-fda-revokes-emergency-use-authorization-chloroquine-and>.
- 632 (30) NIH. NIH Halts Clinical Trial of Hydroxychloroquine. <https://www.nih.gov/news-events/news-releases/nih-halts-clinical-trial-hydroxychloroquine>.
- 633 (31) Chen, G.; Wu, D.; Guo, W.; Cao, Y.; Huang, D.; Wang, H.;
634 Wang, T.; Zhang, X.; Chen, H.; Yu, H.; Zhang, X.; Zhang, M.; Wu, S.;
635 Song, J.; Chen, T.; Han, M.; Li, S.; Luo, X.; Zhao, J.; Ning, Q. Clinical
636 and immunologic features in severe and moderate Coronavirus
637 Disease 2019. *J. Clin. Invest.* **2020**, *130* (5), 2620–2629.
- 638 (32) Wang, X.; Xu, W.; Hu, G.; Xia, S.; Sun, Z.; Liu, Z.; Xie, Y.;
639 Zhang, R.; Jiang, S.; Lu, L. SARS-CoV-2 infects T lymphocytes
640 through its spike protein-mediated membrane fusion. *Cell. Mol.*
641 *Immunol.* **2020**, DOI: 10.1038/s41423-020-0424-9.
- 642 (33) Amici, C.; Di Caro, A.; Ciucci, A.; Chiappa, L.; Castilletti, C.;
643 Martella, V.; Decaro, N.; Buonavoglia, C.; Capobianchi, M. R.;
644 Santoro, M. G. Indomethacin has a potent antiviral activity against
645 SARS coronavirus. *Antivir. Ther.* **2006**, *11* (8), 1021–30.
- 646 (34) Xu, T.; Gao, X.; Wu, Z.; Selinger, W.; Zhou, Z. Indomethacin
647 has a potent antiviral activity against SARS CoV-2 in vitro and canine
648 coronavirus in vivo. *bioRxiv* **2020**, DOI: 10.1101/2020.04.01.017624.
- 649 (35) Castillo, R. R.; Quizon, G. R. A.; Juco, M. J. M.; Roman, A. D.
650 E.; De Leon, D. G.; Punzalan, F. E. R.; Guingon, R. B. L.; Morales, D.
651 D.; Tan, D.-X.; Reiter, R. J. Melatonin as adjuvant treatment for
652 coronavirus disease 2019 pneumonia patients requiring hospital-
653 ization (MAC-19 PRO): a case series. *Melatonin Res.* **2020**, *3* (3),
654 297–310.
- 655 (36) Boga, J. A.; Coto-Montes, A.; Rosales-Corral, S. A.; Tan, D. X.;
656 Reiter, R. J. Beneficial actions of melatonin in the management of viral
657 infections: a new use for this "molecular handyman"? *Rev. Med. Virol.*
658 **2012**, *22* (5), 323–38.
- 659 (37) Wang, D.; Hu, B.; Hu, C.; Zhu, F.; Liu, X.; Zhang, J.; Wang, B.;
660 Xiang, H.; Cheng, Z.; Xiong, Y.; Zhao, Y.; Li, Y.; Wang, X.; Peng, Z.
661 Clinical characteristics of 138 hospitalized patients with 2019 novel
662 coronavirus-infected pneumonia in Wuhan, China. *JAMA* **2020**, *323*
663 (11), 1061–1069.
- (38) Ramamoorthy, S.; Cidlowski, J. A. Corticosteroids: Mecha- 668
669 nisms of action in health and disease. *Rheum. Dis. Clin. North. Am.* 669
670 **2016**, *42* (1), 15–31. 670
- (39) Li, H.; Chen, C.; Hu, F.; Wang, J.; Zhao, Q.; Gale, R. P.; Liang, 671
672 Y. Impact of corticosteroid therapy on outcomes of persons with
673 SARS-CoV-2, SARS-CoV, or MERS-CoV infection: a systematic
674 review and meta-analysis. *Leukemia* **2020**, *34* (6), 1503–1511. 674
- (40) Horby, P.; Lim, W. S.; Emberson, J.; Mafham, M.; Bell, J.; 675
676 Linsell, L.; Staplin, N.; Brightling, C.; Ustianowski, A.; Elmahi, E.;
677 et al. *medRxiv* **2020**, DOI: 10.1101/2020.06.22.20137273. 677
- (41) Lasso, G.; Mayer, S. V.; Winkelmann, E. R.; Chu, T.; Elliot, O.; 678
679 Patino-Galindo, J. A.; Park, K.; Rabadan, R.; Honig, B.; Shapira, S. D.
680 A structure-informed atlas of human-virus interactions. *Cell* **2019**, *178*
681 (6), 1526–1541.e16. 681
- (42) Zhao, Y.; Ren, J.; Harlos, K.; Jones, D. M.; Zeltina, A.; Bowden, 682
683 T. A.; Padilla-Parra, S.; Fry, E. E.; Stuart, D. I. Toremifene interacts
684 with and destabilizes the Ebola virus glycoprotein. *Nature* **2016**, *535*
685 (7610), 169–172. 685
- (43) Johansen, L. M.; Brannan, J. M.; Delos, S. E.; Shoemaker, C. J.; 686
687 Stossel, A.; Lear, C.; Hoffstrom, B. G.; Dewald, L. E.; Schornberg, K.
688 L.; Scully, C.; Lehar, J.; Hensley, L. E.; White, J. M.; Olinger, G. G.
689 FDA-approved selective estrogen receptor modulators inhibit Ebola
690 virus infection. *Sci. Transl. Med.* **2013**, *5* (190), 190ra79. 690
- (44) Cong, Y.; Hart, B. J.; Gross, R.; Zhou, H.; Frieman, M.; 691
692 Bollinger, L.; Wada, J.; Hensley, L. E.; Jahrling, P. B.; Dyall, J.;
693 Holbrook, M. R. MERS-CoV pathogenesis and antiviral efficacy of
694 licensed drugs in human monocyte-derived antigen-presenting cells.
695 *PLoS One* **2018**, *13* (3), No. e0194868. 695
- (45) Dyall, J.; Coleman, C. M.; Hart, B. J.; Venkataraman, T.; 696
697 Holbrook, M. R.; Kindrachuk, J.; Johnson, R. F.; Olinger, G. G., Jr.;
698 Jahrling, P. B.; Laidlaw, M.; Johansen, L. M.; Lear-Rooney, C. M.;
699 Glass, P. J.; Hensley, L. E.; Frieman, M. B. Repurposing of clinically
700 developed drugs for treatment of Middle East respiratory syndrome
701 coronavirus infection. *Antimicrob. Agents Chemother.* **2014**, *58* (8),
702 4885–93. 702
- (46) Kim, Y. I.; Kim, S. G.; Kim, S. M.; Kim, E. H.; Park, S. J.; Yu, K. 703
704 M.; Chang, J. H.; Kim, E. J.; Lee, S.; Casel, M. A. B.; Um, J.; Song, M.
705 S.; Jeong, H. W.; Lai, V. D.; Kim, Y.; Chin, B. S.; Park, J. S.; Chung, K.
706 H.; Foo, S. S.; Poo, H.; Mo, I. P.; Lee, O. J.; Webby, R. J.; Jung, J. U.;
707 Choi, Y. K. Infection and rapid transmission of SARS-CoV-2 in
708 ferrets. *Cell Host Microbe* **2020**, *27* (5), 704–709. 708
- (47) Valavaara, R.; Pyrhonen, S.; Heikkinen, M.; Rissanen, P.; 709
710 Blanco, G.; Tholix, E.; Nordman, E.; Taskinen, P.; Holsti, L.; Hajba,
711 A. Toremifene, a new antiestrogenic compound, for treatment of
712 advanced breast cancer. Phase II study. *Eur. J. Cancer Clin. Oncol.*
713 **1988**, *24* (4), 785–90. 713
- (48) Thompson, I. M., Jr.; Leach, R. Prostate cancer and prostatic 714
715 intraepithelial neoplasia: true, true, and unrelated? *J. Clin. Oncol.*
716 **2013**, *31* (5), 515–6. 716
- (49) Kivinen, S.; Maenpaa, J. Effect of toremifene on clinical 717
718 chemistry, hematology and hormone levels at different doses in
719 healthy postmenopausal volunteers: phase I study. *J. Steroid Biochem.*
720 **1990**, *36* (3), 217–220. 720
- (50) Liu, J.; Cao, R.; Xu, M.; Wang, X.; Zhang, H.; Hu, H.; Li, Y.; 721
722 Hu, Z.; Zhong, W.; Wang, M. Hydroxychloroquine, a less toxic
723 derivative of chloroquine, is effective in inhibiting SARS-CoV-2
724 infection in vitro. *Cell Discovery* **2020**, *6*, 16. 724
- (51) Chen, Z.; Hu, J.; Zhang, Z.; Jiang, S.; Han, S.; Yan, D.; Zhuang, 725
726 R.; Hu, B.; Zhang, Z. Efficacy of hydroxychloroquine in patients with
727 COVID-19: results of a randomized clinical trial. *medRxiv* **2020**,
728 DOI: 10.1101/2020.03.22.20040758. 728
- (52) Chorin, E.; Dai, M.; Shulman, E.; Wadhvani, L.; Bar Cohen, 729
730 R.; Barbhuiya, C.; Aizer, A.; Holmes, D.; Bernstein, S.; Soinelli, M.;
731 Park, D. S.; Chinitz, L.; Jankelsohn, L. The QT interval in patients with
732 SARS-CoV-2 infection treated with hydroxychloroquine/azithromy-
733 cin. *medRxiv* **2020**, DOI: 10.1101/2020.04.02.20047050. 733
- (53) Rajeshkumar, N. V.; Yabuuchi, S.; Pai, S. G.; Maitra, A.; 734
735 Hidalgo, M.; Dang, C. V. Fatal toxicity of chloroquine or 735

736 hydroxychloroquine with metformin in mice. *bioRxiv* **2020**,
737 DOI: 10.1101/2020.03.31.018556.
738 (54) Gassen, N. C.; Niemeyer, D.; Muth, D.; Corman, V. M.;
739 Martinelli, S.; Gassen, A.; Hafner, K.; Papias, J.; Mosbauer, K.;
740 Zellner, A.; Zannas, A. S.; Herrmann, A.; Holsboer, F.; Brack-Werner,
741 R.; Boshart, M.; Muller-Myhsok, B.; Drosten, C.; Muller, M. A.; Rein,
742 T. SKP2 attenuates autophagy through Beclin1-ubiquitination and its
743 inhibition reduces MERS-Coronavirus infection. *Nat. Commun.* **2019**,
744 *10* (1), 5770.
745 (55) Shi, J.; Wen, Z.; Zhong, G.; Yang, H.; Wang, C.; Huang, B.; Liu,
746 R.; He, X.; Shuai, L.; Sun, Z.; Zhao, Y.; Liu, P.; Liang, L.; Cui, P.;
747 Wang, J.; Zhang, X.; Guan, Y.; Tan, W.; Wu, G.; Chen, H.; Bu, Z.
748 Susceptibility of ferrets, cats, dogs, and other domesticated animals to
749 SARS-coronavirus 2. *Science* **2020**, 368 (6494), 1016–1020.